Materials Research Proceedings 44 (2024) 106-112 https://doi.org/10.21741/9781644903254-12

Simulation of texture-related micro-indentation behavior of typical HCP alloy plates

ZHOU Xiangyu[1,a], ZHOU Kecheng[1,b], WU Peidong[2,c], XU Zhutian[1,d], PENG Linfa[1,e] *, LI Shuhui[1,f] and WANG Huamiao[1,3,g] *

[1]State Key Laboratory of Mechanical System and Vibration, Shanghai Jiao Tong University, Shanghai, 200240, China

[2]Department of Mechanical Engineering, McMaster University, Hamilton, ON, Canada, L8S 4L7

[3]School of Mechanics and Engineering Science, Shanghai University, Shanghai, 200072, China

[a]sjtuzhouxy@sjtu.edu.cn, [b]kecheng@sjtu.edu.cn, [c]peidong@mcmaster.ca, [d]zhutianxu@sjtu.edu.cn, [e]penglinfa@sjtu.edu.cn, [f]lishuhui@sjtu.edu.cn, [g]wanghm@shu.edu.cn

Keywords: Magnesium Alloy, Texture-Dependency, Crystal Plasticity, Twinning

Abstract: The mechanical behaviors of magnesium and its alloys, regulated by the slip and twinning mechanisms, are remarkably influenced by the crystalline orientation. A better understanding and quantification of the mechanisms in deformation is necessary. To this end, the crystal plasticity finite element (CPFE) simulations of magnesium alloy plates have been investigated in this study. The process of impression of single crystal samples with three different declination angles with 0°, 45°, and 90° is simulated. The corresponding detailed CPFE simulations reveal a texture-dependent spatial distribution of extension twins, and the twin morphologies and the indentation topography of single crystals have been discussed, highlighting the influence of the initial texture. Furthermore, the simulations uncover the accumulated shear strain of the deformation system varying with spatial position inside the sample, which is in favor of the analysis of the twin-favor zone.

Introduction

In the context of the pursuit of the low-carbon economy, magnesium and its alloys have triggered worldwide attention because of their lightweight, high specific strength, and excellent recyclability [1–4]. The strong anisotropic mechanical behavior of Mg alloys, influenced by the hexagonal close-packed (HCP) structure, the intrinsic polarity of the twin, and the crystal orientation [5–8], is currently a hindrance to their potential prevalent applications. To address this issue, a better understanding and quantification of the competition among the predominant microscopic mechanisms that govern the mechanical behavior of Mg alloys is crucial, particularly in regard to the role of the initial texture in shaping these mechanisms. At room temperature, slip and extension twin [9–13] are the major mechanisms behind the plastic deformation. Numerous studies have investigated the mechanical behaviors and underlying microscopic mechanisms of Mg alloys under homogeneous loading conditions [14–17] such as tension, compression, and simple shear, as well as inhomogeneous loading conditions like torsion [18,19] and bending [20,21].

The indentation test is a widely used method for determining the mechanical properties of materials, where the complexity of the stress state around an indenter may sophisticate the interactions between the various deformation modes. But there is much less fundamental understanding regarding the nature of plastic deformation activity especially the extension twin under such localized loading conditions. Gollapudi et al. [22] experimentally concurred that the extension twin and basal slip are responsible for the crystal-orientation dependent indentation morphologies of Mg alloy. Shin et al. [23] conducted nanoindentation on the basal and prismatic planes of single-crystalline Mg and found that extension twin is essential for strain

Content from this work may be used under the terms of the Creative Commons Attribution 3.0 license. Any further distribution of this work must maintain attribution to the author(s) and the title of the work, journal citation and DOI. Published under license by Materials Research Forum LLC.

accommodation. Bočan et al. [24] found a strong correlation between the nanomechanical behaviors of pure Mg and AZ31 alloy and the crystal orientation, which can be interpreted by the anisotropic activities of slip systems and extension twin.

Moreover, the means of the crystal plastic finite element (CPFE) method was employed for the interpretation of the indentation behaviors of magnesium, which provides easy access to factors that are difficult to obtain experimentally. Kitahara et al. [25] reported the twin morphologies beneath indent on low index planes in pure Mg single crystals and they concluded that the anisotropic development of the twin region is induced by the basal slip through CPFE simulations. Sánchez-Martín et al. [26] studied the activation and propagation of twinning in pure Mg grains with different orientations. The crystal-orientation dependent indentation topographies driven by the activity of extension twin have been observed in experiments and confirmed by CPFE simulations. Zambaldi et al. [27] presented the crystal-orientation dependent response of pure Mg during single-grain indentation. The importance of the twinning behaviors is emphasized in their research, but hardly a visually apparent twin distribution inside the sample can be found. Besides, the indentation behaviors and underly microscopic mechanisms of polycrystalline Mg alloys should be further investigated, especially the twin pattern. In the following, twin nucleation, propagation, and growth (TNPG) model [28] has been employed in a CPFE method to describe the twinning mechanism and analyze the indentation behavior of single crystal samples and randomly oriented sample. The texture-dependent indentation behaviors will be discussed.

Numerical procedures

Description of Crystal Plasticity Model. The CPFEM for indentation of polycrystalline Mg alloy in this paper can be found else wise [29]. It is briefly described for completeness. For both slip and twinning systems, the shear rate ($\dot{\gamma}^{\alpha}$) is formulated as

$$\dot{\gamma}^{\alpha} = \dot{\gamma}_0 \left|\frac{\tau^{\alpha}}{\tau_c^{\alpha}}\right|^{\frac{1}{m}} sgn(\tau^{\alpha}) \tag{1}$$

where $\dot{\gamma}_0$, m, τ^{α}, and τ_c^{α} refer to reference shear rate, rate sensitivity component, resolved shear stress (RSS), and critical resolved shear stress (CRSS), respectively. The evolution of CRSS in the deformation process is given by

$$\dot{\tau_c^{\alpha}} = \frac{d\hat{\tau}^{\alpha}}{d\Gamma} \sum_{\beta} h^{\alpha\beta} \left|\dot{\gamma}^{\beta}\right| \tag{2}$$

where Γ, $h^{\alpha\beta}$, $\hat{\tau}^{\alpha}$ are the accumulated shear strain in the grain ($\Gamma = \sum_{\alpha} \int \dot{\gamma}^{\alpha} dt$), the hardening coupling coefficients, which used to describe the resistance on system α associated with system β, and the threshold stress, respectively.

The threshold stress for a slip system α is related to the initial CRSS (τ_0^{α}), the back-extrapolated CRSS ($\tau_0^{\alpha} + \tau_1^{\alpha}$), the initial hardening rate (h_0^{α}), and the asymptotic hardening rate (h_1^{α}) in an extended Voce law.

$$\hat{\tau}^{\alpha} = \tau_0^{\alpha} + (\tau_1^{\alpha} + h_1^{\alpha}\Gamma)\left(1 - \exp\left(-\frac{h_0^{\alpha}}{\tau_1^{\alpha}}\Gamma\right)\right) \tag{3}$$

The stress relaxation associated with twinning is accounted for by employing the model proposed by Wu et al. [30], where the threshold stress for twinning system α is

$$\hat{\tau}^{\alpha} = \begin{cases} \tau_0^{\alpha} - \frac{\tau_0^{\alpha} - \tau_g^{\alpha}}{f_g^{\alpha}} f^{\alpha} & f^{\alpha} \le f_g^{\alpha} \\ \tau_0^{\alpha} + (\tau_1^{\alpha} + h_1^{\alpha}\Gamma)\left(1 - \exp\left(-\frac{h_0^{\alpha}}{\tau_1^{\alpha}}\Gamma\right)\right) & f^{\alpha} > f_g^{\alpha} \end{cases} \tag{4}$$

Materials Research Proceedings 44 (2024) 106-112 https://doi.org/10.21741/9781644903254-12

where f_g^α is the critical twin volume fraction, τ_g^α is the minimum twin resistance and f^α is the current twin volume fraction (TVF). Twinning is terminated within a grain if the TVF reaches a threshold value V^{th}.

Finite Element Model. The crystal plasticity finite element (FE) simulation was performed using ABAQUS v2022, a commercial software package. Fig. 1 shows the schematic diagram of models with three different declination angles: (I) 0°, (II) 45° and (III) 90°. To facilitate the following discussion, each model is divided into four parts based on the symmetry of the Vickers indenter: northern west (NW), northern east (NE), southern west (SW), and southern east (SE). The single crystal constitutive model described earlier was implemented in the ABAQUS UMAT subroutine to describe the constitutive response at every integration point of all elements.

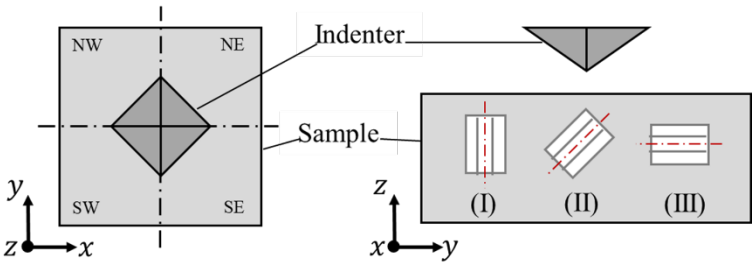

Fig. 1. The schematic diagram of indentation test model.

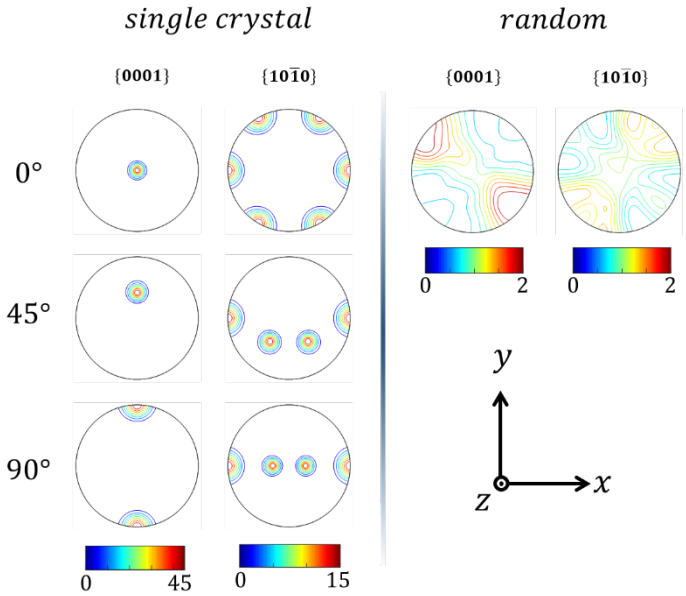

Fig. 2. The pole figures of indentation samples in terms of $\{\mathbf{0001}\}$ *and* $\{\mathbf{10\bar{1}0}\}$.

The pole figures of single crystal and random samples are presented in Fig. 2. To simulate the plastic deformation behavior of different samples, the crystal orientation information was incorporated into the crystal plasticity subroutine. Each element, which represents a single grain, was assigned a set of Euler angles to define its crystal orientation. Basal slip, prismatic slip, and pyramidal slip, and extension twin were considered in the modeling to accommodate the plastic deformation.

Results and discussion

Twin Morphologies. Fig. 3(a-c) show the simulated twin morphologies of the 0°, 45°, and 90° indentation samples. These morphologies correspond to the set of nodes where the TVF (Twinning Volume Fraction) is greater than 0.1. In the 0° sample, the twins are mainly concentrated in the

Materials Research Proceedings 44 (2024) 106-112 https://doi.org/10.21741/9781644903254-12

region that interfaces directly with the indenter and are confined to shallow layers. Conversely, the extension twin in the 45° and 90° samples is more extensive and penetrates deeper beneath the indenter-contact area. The convex hull formed by the twins has a distinct angular morphology and exhibits strong symmetry. In the case of single crystal-0, the indentation results show a hexagram-like pattern, which is associated with the six variants of the extension twin [30]. In the case of the single crystal-45 sample, the twin distribution mainly penetrates into the northern part of the sample, and the distribution of twins in this sample displays better symmetry with respect to the x=0 plane, as is also observed in the single crystal-90 sample.

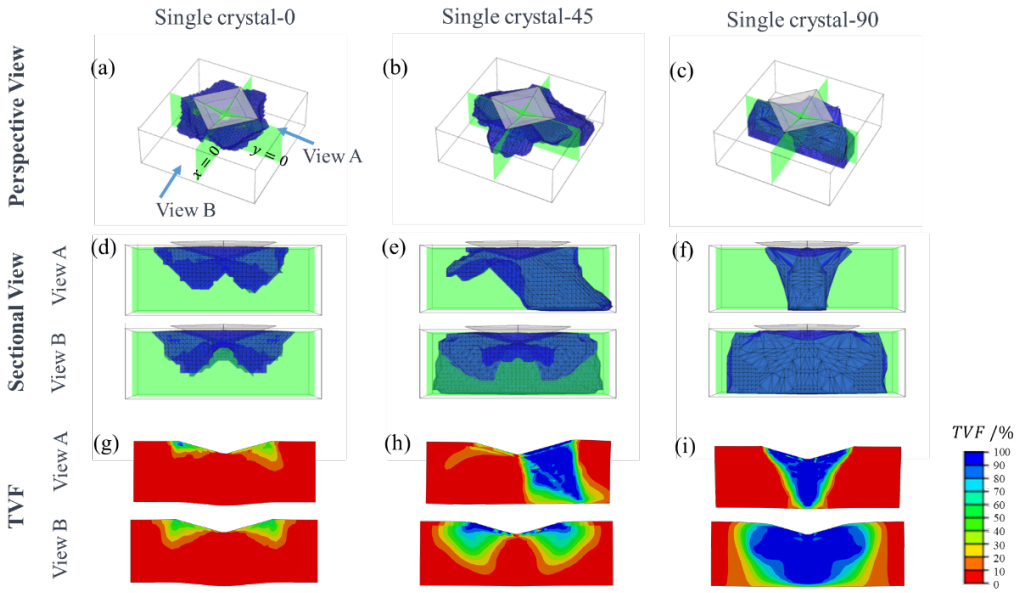

Fig. 3. The simulated 3D-twin morphology of (a) single cyrstal-0, (b) single crystal-45, and (c) single cyrstal-90 sample, (d–f) The 2D-twin morphology at x=0 section and y=0 section, (g–i) The TVF distribution at $\boldsymbol{x = 0}$ *section and* $\boldsymbol{y = 0}$ *section.*

Accumulated Shear Strain. Fig. 4 presents a comparison of the accumulated shear strain distribution between the simulated results of single crystal samples with different initial orientations and random sample. In single crystal 0 sample, basal slip is found to be the dominant deformation mechanism. Specifically, the accumulated shear strain resulting from basal slip increases to a maximum at approximately 20 microns and then decreases gradually. The accumulated shear strain of extension twin monotonically decreases from the surface. In contrast, a significant difference is evident between the northern part (NW, NE) and the southern part (SW, SE) in the accumulated shear strain of basal slip and extension twin in single crystal-45 sample, as illustrated in Fig. 4(b). The shear strain of the extension twin is conspicuously higher in the northern part compared to the southern part, resulting in the anisotropic distribution of the twin region (Fig. 3(e, h)). The shear strain of basal slip in the northern part is also higher than that in the southern part. Due to the symmetry of twin regions, a similar distribution pattern of shear strain also observed in the single crystal-90 sample, as shown in Fig. 3(f, i).

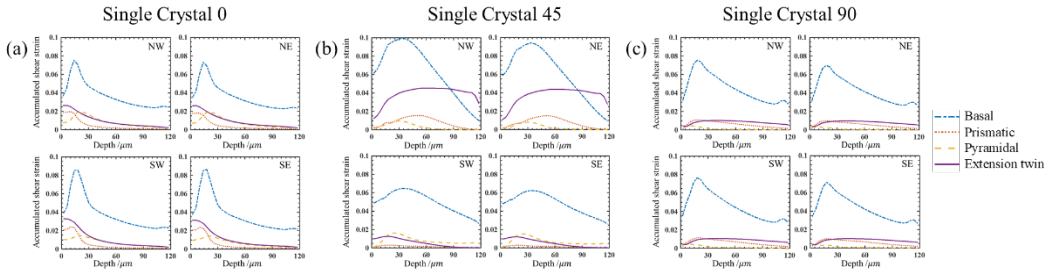

Fig. 4. The accumulated shear strain distribution along depth of basal slip, prismatic slip, pyramidal slip, and extension twin: (a) single crystal-0 sample, (b) single crystal-45 sample and (c) single crystal-90 sample.

The Indentation Morphology. Fig. 5 depicts the simulated indentation morphology of four samples. As shown in Fig. 5(d), no pile-up or sink-in effects are observed in random sample. In contrast, the texture-dependent indentation morphologies of single crystal samples (Fig. 5(a-c)) are highlighted. The single crystal samples exhibit smooth raised features on their surface. In the single crystal-0 samples, the pile-up profile occurs adjacent to the indenter. In the single crystal-45 samples, the pile-up profile is observed in the northern part, and the sink-in profile occurs around the indenter and expands along the x-axis. In the single crystal-90 sample, the pile-up profile is marginally apparent and the expansion of sink-in profile is more prominent. Notably, the extension twin in the samples can cause apparent extension along the c-axis and shrinkage perpendicular to the c-axis, resulting in pile-up and sink-in effects observed in the indentation morphology. Therefore, the twin morphology can be inferred from the indentation morphology, and vice versa.

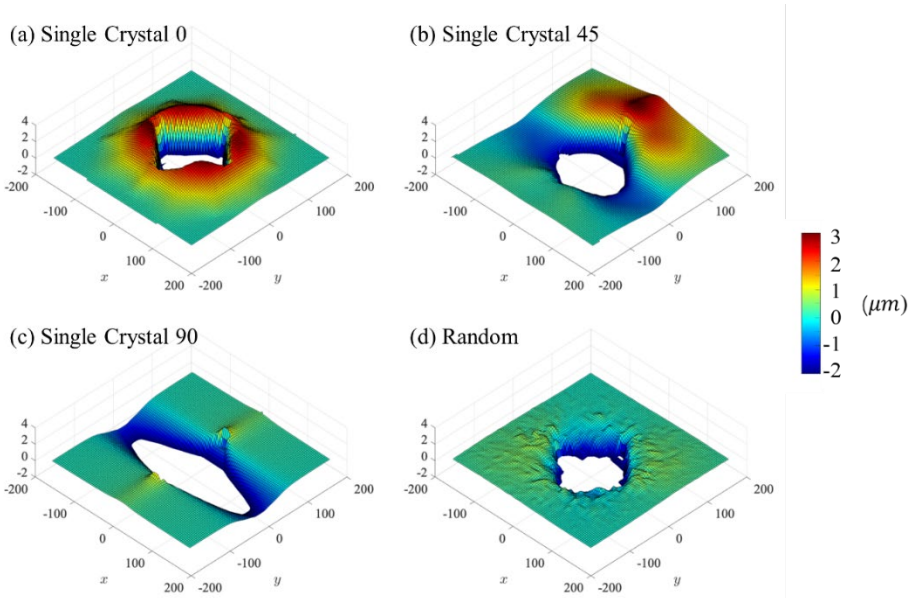

Fig. 5. The simulated indentation morphology of (a–c) single crystal texture samples, and (d) random texture sample.

Summary and Conclusions

In this work, three-dimensional crystal plasticity finite element (CPFE) simulations were performed using several initial textures, including three single crystal textures, and a random texture. The 3-D and 2-D twin morphologies, surface morphologies and accumulated shear strain of deformation mode are discussed, and they all show texture-dependent characteristics. The surface morphologies are strongly correlated with the internal twin distribution. Additionally, the

shear strain distribution of the extension twin corresponds to its three-dimensional twin distribution. In the single crystal-0 sample, twin is confined to the shallow layer, but it can penetrate deep beneath the region directly under the indenter in the single crystal-90 sample. As for the single crystal-45 sample, the twin only extends into the northern parts.

References

[1] S.R. Agnew, J.F. Nie, Preface to the viewpoint set on: The current state of magnesium alloy science and technology, Scr. Mater. 63 (2010) 671–673. https://doi.org/10.1016/j.scriptamat.2010.06.029

[2] D. Eliezer, E. Aghion, F.H. (Sam) Froes, Magnesium Science, Technology and Applications, Adv. Perform. Mater. 5 (1998) 201–212. https://doi.org/10.1023/A:1008682415141.

[3] T.M. Pollock, Weight Loss with Magnesium Alloys, Science. 328 (2010) 986–987. https://doi.org/10.1126/science.1182848

[4] Y. Yang, X. Xiong, J. Chen, X. Peng, D. Chen, F. Pan, Research advances in magnesium and magnesium alloys worldwide in 2020, J. Magnes. Alloy. 9 (2021) 705–747. https://doi.org/10.1016/j.jma.2021.04.001

[5] B. Shi, C. Yang, Y. Peng, F. Zhang, F. Pan, Anisotropy of wrought magnesium alloys: A focused overview, J. Magnes. Alloy. 10 (2022) 1476–1510. https://doi.org/10.1016/j.jma.2022.03.006

[6] C.M. Cepeda-Jiménez, M.T. Pérez-Prado, Microplasticity-based rationalization of the room temperature yield asymmetry in conventional polycrystalline Mg alloys, Acta Mater. 108 (2016) 304–316. https://doi.org/10.1016/j.actamat.2016.02.023

[7] Y.B. Chun, C.H.J. Davies, Twinning-induced anomaly in the yield surface of highly textured Mg–3Al–1Zn plate, Scr. Mater. 64 (2011) 958–961. https://doi.org/10.1016/j.scriptamat.2011.01.044

[8] H. Qiao, X.Q. Guo, A.L. Oppedal, H. El Kadiri, P.D. Wu, S.R. Agnew, Twin-induced hardening in extruded Mg alloy AM30, Mater. Sci. Eng., A. 687 (2017) 17–27. https://doi.org/10.1016/j.msea.2016.12.123

[9] C.S. Roberts, Magnesium and its Alloys, John Wiley & Sons, Inc., New York, 1960. https://doi.org/10.1002/9781118985960.meh107

[10] F.E. Hauser, P.R. Landon, J.E. Dorn, Deformation and fracture mechanisms of polycrystalline magnesium at low temperatures, Transactions of American Society for Metals. 48 (1956) 986–1002.

[11] E.C. Burke, W.R. Hibbard, Plastic Deformation of Magnesium Single Crystals, JOM. 4 (1952) 295–303. https://doi.org/10.1007/BF03397694

[12] R.E. Reed-Hill, W.D. Robertson, Pyramidal slip in magnesium, Trans. TMS-AIME. 212 (1958) 256–259.

[13] E.W. Kelley, W.F. Hosford, Plane-strain compression of magnesium and magnesium alloy crystals, Trans Met Soc AIME. 242 (1968) 5–13.

[14] X. Lou, M. Li, R. Boger, S. Agnew, R. Wagoner, Hardening evolution of AZ31B Mg sheet, Int. J. Plast. 23 (2007) 44–86. https://doi.org/10.1016/j.ijplas.2006.03.005

[15] H. Wang, Y. Wu, P.D. Wu, K.W. Neale, Numerical analysis of large strain simple shear and fixed-end torsion of HCP polycrystals, Comput. Mater. Contin. 19 (2010) 255. https://doi.org/10.3970/cmc.2010.019.255

[16] H. Wang, B. Raeisinia, P.D. Wu, S.R. Agnew, C.N. Tomé, Evaluation of self-consistent polycrystal plasticity models for magnesium alloy AZ31B sheet, Int. J. Solids Struct. 47 (2010) 2905–2917. https://doi.org/10.1016/j.ijsolstr.2010.06.016

[17] M. Sabbaghian, N. Fakhar, P. Nagy, K. Fekete, J. Gubicza, Investigation of shear and tensile mechanical properties of ZK60 Mg alloy sheet processed by rolling and sheet extrusion, Mater. Sci. Eng., A. 828 (2021) 142098. https://doi.org/10.1016/j.msea.2021.142098

[18] P.D. Wu, H. Wang, K.W. Neale, On the large strain torsion of HCP polycrystals, Int. J. Appl. Mechanics. 04 (2012) 1250024. https://doi.org/10.1142/S175882511250024X

[19] H. Wang, X. Zhang, W. Wu, P.K. Liaw, K. An, Q. Yu, P. Wu, On the torsional and coupled torsion-tension/compression behavior of magnesium alloy solid rod: A crystal plasticity evaluation, Int. J. Plast. 151 (2022) 103213. https://doi.org/10.1016/j.ijplas.2022.103213

[20] D. Tang, K. Zhou, W. Tang, P. Wu, H. Wang, On the inhomogeneous deformation behavior of magnesium alloy beam subjected to bending, Int. J. Plast. 150 (2022) 103180. https://doi.org/10.1016/j.ijplas.2021.103180

[21] K. Zhou, X. Sun, H. Wang, X. Zhang, D. Tang, W. Tang, Y. Jiang, P. Wu, H. Wang, Texture-dependent bending behaviors of extruded AZ31 magnesium alloy plates, J. Magnes. Alloy (2023) S2213956723000294. https://doi.org/10.1016/j.jma.2023.02.003

[22] S. Gollapudi, M.A. Azeem, A. Tewari, U. Ramamurty, Orientation dependence of the indentation impression morphology in a Mg alloy, Scr. Mater. 64 (2011) 189–192. https://doi.org/10.1016/j.scriptamat.2010.09.041

[23] J.-H. Shin, S.-H. Kim, T.K. Ha, K.H. Oh, I.-S. Choi, H.N. Han, Nanoindentation study for deformation twinning of magnesium single crystal, Scr. Mater. 68 (2013) 483–486. https://doi.org/10.1016/j.scriptamat.2012.11.030

[24] J. Bočan, J. Maňák, A. Jäger, Nanomechanical analysis of AZ31 magnesium alloy and pure magnesium correlated with crystallographic orientation, Mater. Sci. Eng. A 644 (2015) 121–128. https://doi.org/10.1016/j.msea.2015.07.055

[25] H. Kitahara, T. Mayama, K. Okumura, Y. Tadano, M. Tsushida, S. Ando, Anisotropic deformation induced by spherical indentation of pure Mg single crystals, Acta Mater. 78 (2014) 290–300. https://doi.org/10.1016/j.actamat.2014.06.039

[26] R. Sánchez-Martín, M.T. Pérez-Prado, J. Segurado, J.M. Molina-Aldareguia, Effect of indentation size on the nucleation and propagation of tensile twinning in pure magnesium, Acta Mater. 93 (2015) 114–128. https://doi.org/10.1016/j.actamat.2015.04.005

[27] C. Zambaldi, C. Zehnder, D. Raabe, Orientation dependent deformation by slip and twinning in magnesium during single crystal indentation, Acta Mater. 91 (2015) 267–288. https://doi.org/10.1016/j.actamat.2015.01.046

[28] P.D. Wu, X.Q. Guo, H. Qiao, D.J. Lloyd, A constitutive model of twin nucleation, propagation and growth in magnesium crystals, Mater. Sci. Eng. A 625 (2015) 140–145. https://doi.org/10.1016/j.msea.2014.11.096

[29] H. Wang, P.D. Wu, J. Wang, C.N. Tomé, A crystal plasticity model for hexagonal close packed (HCP) crystals including twinning and de-twinning mechanisms, Int. J. Plast. 49 (2013) 36–52. https://doi.org/10.1016/j.ijplas.2013.02.016

[30] B. Selvarajou, J.-H. Shin, T.K. Ha, I. Choi, S.P. Joshi, H.N. Han, Orientation-dependent indentation response of magnesium single crystals: Modeling and experiments, Acta Mater. 81 (2014) 358–376. https://doi.org/10.1016/j.actamat.2014.08.042